Discussion Document in preparation of the 11^{th} Coordination Meeting of the ORM Study
March 2^{nd}, 2000 – ESA Headquarters – Paris (France)

Mapping of Temperature and Line-of-Sight Errors in Constituent Retrievals for MIPAS / ENVISAT Measurements

Firenze, 22 February 2000

Prepared by: Marco Ridolfi* and Piera Raspollini

---

1. INTRODUCTION

In the ORM code, line of sight (i.e. tangent pressure, p) and temperature (T) are retrieved simultaneously among themselves, but sequentially with respect to the volume mixing ratio of the five key species. The sequential retrieval leaves unaccounted the mapping of line of sight and temperature errors in the retrieved volume mixing ratio (VMR) of the constituents. Therefore, this error contribution must be evaluated *a-posteriori* , using a dedicated algorithm.

2. OBJECTIVE

Scope of the present document is to briefly recall the principles of the algorithm that allows for an *a-posteriori* evaluation of pT induced error on VMR retrievals.
Since the last co-ordination meeting of the ORM study held in Bologna on November 11^{th}, 1999, further investigations regarding pT error propagation in MIPAS VMR retrievals have been carried-out. In particular, the variability of this error source as a function of observation geometry, latitude and atmospheric model was analyzed. The results of these analyses are summarized in the present document.

3. MAPPING OF p,T ERROR ON VMR RETRIEVAL (THEORY)

At each Newtonian iteration *iter* the VMR retrieval algorithm updates the VMR profile $\mathbf{x}_{iter}$ using the inversion formula (see e.g. Rodgers, 1976 and Ridolfi et al., 1999):

$$\mathbf{x}_{iter} = \mathbf{x}_{iter-1} + \left(\mathbf{K}^T\mathbf{V}_{obs.}^{-1}\mathbf{K}\right)^{-1}\mathbf{K}^T\mathbf{V}_{obs.}^{-1}\mathbf{n} \equiv \mathbf{Dn} \tag{1}$$

where $\mathbf{n}$ is the so called 'residuals' vector containing the differences between observations and the current simulations, $\mathbf{K}$ is the Jacobian of the retrieval containing the derivatives of the simulated spectra with respect to the unknown parameters and $\mathbf{V}_{obs.}$ is the VCM relating to the random error on the observations. The matrix:

$$\mathbf{V}_{\mathbf{x}} = \left(\mathbf{K}^T\mathbf{V}_{obs.}^{-1}\mathbf{K}\right)^{-1} \tag{2}$$

represents the VCM of the retrieved VMR profile due to measurement noise.

---

* IROE - CNR Via Panciatichi, 64 I-50127 Firenze (Italy)

An erroneous estimate of tangent pressure and temperature leads to further error affecting the retrieved VMR. Namely, an uncertainty on the assumed tangent pressures and temperatures characterized by a VCM $\mathbf{V}_{PT}$ translates on to an error on the simulated spectra and therefore on to an error on the retrieved VMR profile characterized the VCM $\mathbf{V}_{\mathbf{x}}'$ given by:

$$\mathbf{V}_{\mathbf{x}}' = \mathbf{D}\mathbf{C}\mathbf{V}_{PT}\mathbf{C}^T\mathbf{D}^T \tag{3}$$

where **D** is the VMR retrieval inversion matrix defined by Eq. (1) and is assumed as locally independent of p,T (always true for small p,T errors), and **C** is the matrix accounting for p,T error propagation in the simulated spectra of VMR retrieval. By definition matrix **C** is equal to:

$$C_{i,j} = \frac{\partial S_i}{\partial (p,T)_j} \tag{4}$$

where S_i is the simulated spectrum (the index '*i*' spans over the simulated points of the spectrum, all the used microwindows and tangent altitudes) and $(p,T)_j$ is a vector that includes both the line of sight parameters and the vertical profile of the atmospheric temperature.

It is important to underline that for a rigorous treatment, in Eq. (1) $\mathbf{V}_{obs.}$ should be replaced by $\mathbf{V}_{obs} + \mathbf{C}\mathbf{V}_{PT}\mathbf{C}^T$. However, assuming that microwindow selection and quality of p,T retrievals make the values of $\mathbf{C}\mathbf{V}_{PT}\mathbf{C}^T$ negligible with respect to those of $\mathbf{V}_{obs}$, Eq. (1) can be adequate for the calculation of $\mathbf{x}_{iter}$ even if concurrent combinations of the errors, that possibly affect $\mathbf{C}\mathbf{V}_{PT}\mathbf{C}^T$ rather than the random errors $\mathbf{V}_{obs}$, can make $\mathbf{V}_{\mathbf{x}}'$ significant with respect to $\mathbf{V}_{\mathbf{x}}$.

Despite the fact that matrix **D** is already calculated by the inversion algorithm, it is unpractical to use matrices **D** and **C** individually for evaluating $\mathbf{V}_{\mathbf{x}}'$, because:

- calculation of matrix **C** is demanding in terms of computing time, therefore it is not an advisable operation for the NRT processor
- storing matrix **C** into a database is a difficult operation given its relatively large size (≈ 2 Mb)

A convenient method for the evaluation of $\mathbf{V}_{\mathbf{x}}'$ is by way of the matrix $\mathbf{E} \equiv \mathbf{D}\mathbf{C}$ that provides directly the mapping of p,T error on to the retrieved VMR:

$$\mathbf{V}_{\mathbf{x}}' = \mathbf{E}\mathbf{V}_{PT}\mathbf{E}^T \tag{5}$$

The calculation of matrix **E** in the on-line processor of MIPAS is a very time consuming operation, however, its dimensions ((32 x 16) in the standard MIPAS measurement scenario) are very small compared to those of matrix **C** and a look-up table of **E** matrices can be easily installed in the ground processor.

The choice of a look-up table must be evaluated in the light of the variability of matrix **E**. Matrix **E** depends on:

- set of spectral microwindows analyzed in VMR retrieval
- temperature vertical profile
- VMR profile of the retrieved species,
- VMR profile of the interfering species
- observation geometry (tangent pressures)

Handling the multiplicity of these dependencies could be a major complication, however as we will show in Sect. 5, the dependencies relating to the atmospheric status can be grouped into a single dependence on latitude and the dependence on tangent pressure can be neglected.

4. SIGNIFICANCE OF p,T INDUCED ERROR IN VMR RETRIEVAL

The p,T error propagation matrix **E** was calculated by means of sensitivity tests for all MIPAS target species, using a standard set of microwindows for data analysis and assuming the U.S. standard mid-latitude spring atmosphere (National Oceanic and Atmospheric Administration et al., 1976) for the generation of the simulated observations. Fig. 1 illustrates the typical structure of matrix **E** in the case of H_2O retrieval. In the horizontal axes we have reported the p,T retrieved parameters index (left side) and the VMR parameter index (right side). In the p,T parameter index axis, indices form 1 to 16 refer to tangent pressures of sweeps with tangent altitude in the range 53, ..., 8 km in 3 km steps (standard MIPAS scan), while the indices from 17 to 32 refer to the temperatures at the same altitudes. In the VMR parameter index axis, the indices from 1 to 16 refer to the VMR corresponding to tangent altitudes 53, ..., 8 km in 3 km steps. In the vertical axis we report the relative VMR error due to 1K temperature error or 1% tangent pressure error.

In Fig. 2 we compare the measurement noise error on the retrieved H_2O (central panel) and CH_4 (right panel) with the error due to propagation of p,T uncertainties. This latter error component was evaluated using Eq. (5) with a $\mathbf{V}_{PT}$ having variances corresponding to the p,T errors reported in the left panel of Fig.2. It is evident that in both cases of H_2O and CH_4, pressure and temperature induced error is significant with respect to the noise error and, at low altitudes, in the H_2O case, this error source may be even much greater than the noise error. In fact, at low altitudes, below the hygropause, the water vapor VMR has a very steep gradient and therefore, even a relatively small error on the evaluation of tangent pressure translates into a relatively large error on the H_2O VMR.

The shape of the matrix **E** shown in Fig. 1 suggests that the dominant contribution to the VMR error at a given altitude arises from the error on pressure and temperature at the same altitude and correlations between parameters at different altitudes may have a secondary role in the p,T error propagation process. In Fig. 3 we show the comparison between p,T induced errors on CH_4 VMR calculated using the full **E** matrix relating to CH_4 retrieval (solid line) and using only the elements of the main diagonals of this matrix (dashed line). In this case, neglecting the correlations among different altitudes implies an inaccuracy in the evaluation of p,T induced errors. This inaccuracy ($\approx$ 20%) is not large but, considering that:

1. neglecting the correlations between different altitudes allows a major reduction of matrix **E** size (from 2 Kb to 0.13 Kb), however the size of the full **E** matrix is very small compared to the size of the other entities to be stored in MIPAS Level 2 ground processor,
2. in our retrieval scheme (global-fit) the VMR profile is simultaneously determined at all tangent altitudes, therefore, the off-diagonal elements of matrix **E** turn-out to be automatically determined when carrying-out the sensitivity tests for the determination of the main diagonals of matrix **E**,

the approximation of neglecting correlations between different altitudes for the determination of p,T induced error does not provide significant savings and will not be used.

5. VARIABILITY OF p,T ERROR PROPAGATION

Accounting for the variability of p,T error propagation matrix **E** is in general a hard task due to the multiplicity of dependencies listed in Sect. 3. In this section we discuss how these dependencies can be handled using a simplified approach.

First, the dependence on the selected set of microwindows analyzed in VMR retrieval has a non-predictable and discontinuous behavior as a function of the used microwindows therefore, a personalized **E** matrix must be calculated for each of the possible sets of microwindows. No simplification is possible in the case of this dependence.

On the other hand, the variability with atmospheric temperature and composition can be summarized as a single dependence on the atmospheric status which, in turn, depends on latitude and season. Let's consider first the latitudinal dependence of p,T error propagation. We assume the latitudinal variability of the atmosphere as described by the model (relating to the month of October) from Rummukainen et al. (1999) and report the results in the case of methane (CH_4). Methane was chosen because it is very sensitive to temperature variations, being the microwindows used to perform the retrieval of its VMR mainly located in the high frequency bands of MIPAS.

Assuming that a scan has been measured at 43° N latitude, the exact procedure for calculating the p,T error propagation in VMR retrievals is to use a matrix **E** evaluated in correspondence of a atmosphere relating to 43° N latitude. The result of such a calculation is reported as a solid line in Fig. 4, panel (a). If the same error is calculated using a propagation matrix **E** relating to a different latitude, the error obtained in this approximation differs from its 'exact' value by an amount that depends on the latitude assumed for the calculation of the used matrix **E**. The dashed curves reported in Fig. 4 represent the p,T induced error calculated using p,T error propagation matrices derived under the assumption of a latitude different from the real latitude of 43° N. The spread among the different curves is significant but not large. This spread can be reduced by reducing the

latitudinal range used for the calculation of the p,T error propagation matrices. In Fig. 4 panel (b), the solid curve (representing the same error reported as a solid curve in Fig. 4 panel (a)) is compared with the errors (dashed curves) calculated with p,T error propagation matrices belonging to a restricted latitude range (from 27° N to 59° N). In this case the spread among the errors calculated with different p,T error propagation matrices is significantly smaller than in Fig. 4 panel (a).
At the current stage it is difficult to establish whether the accuracy of the p,T induced error obtained in the panel (b) of Fig. 4 using a latitude discretization of about 30 degrees is satisfactory or not. In fact, the answer to this question depends very much on the relative contribution of p,T induced error to the total VMR error budget, whose estimate in turn depends on some critical choices that are still pending. Possibly, a latitude discretization of at least 30 degrees will be used, however, if necessary, a finer tabulation step can be chosen for the propagation matrix **E** in order to reduce the uncertainty on p,T induced error to acceptable values.
Besides latitudinal variations, the seasonal variability of the atmosphere could be an important factor limiting the accuracy of the estimated p,T induced error. In order to evaluate the impact of this type of variability we have evaluated the p,T induced error on CH_4 VMR for a few different atmospheric models relating to the same latitude of about 45 degrees and different seasons. In Fig. 5, the p,T induced error on CH_4 VMR calculated with a p,T error propagation matrix **E** relating to the mid-latitude U.S. standard atmosphere (solid line) is compared with the estimates of the same error obtained using **E** matrices relating to different atmospheres, namely: the FASCOD2 Mid-latitude summer and winter atmospheres (Anderson et al., 1986) and the Rummukainen et al. (1999) 43° N and 43° S October atmospheres. The spread of the curves reported in Fig. 5, representing the accuracy of the p,T induced error estimate, is very similar to the spread obtained in Fig. 4 panel (b) for the case of the latitudinal variability in a 30 degrees latitude interval. As for the case of the latitudinal variability, also in the case of seasonal variability, presently it is not possible to establish whether the accuracy of p,T induced error estimate attained in Fig. 5 is satisfactory or not. Possibly the season dependence will be neglected, however, if the accuracy attained by neglecting the seasonal variability is not satisfactory, a tabulation of the p,T error propagation matrix **E** in the 2-D domain of latitude and season may be considered.
Finally, a test was carried-out in order to assess the entity of the dependence of **E** matrix on the observation geometry. The p,T induced error on the CH_4 VMR measured with the standard MIPAS scan was calculated using **E** matrices relating to different scan patterns. In Fig. 6 we compare the p,T induced error on the CH_4 VMR calculated with **E** matrices relating to the standard scan pattern (solid line), to a scan pattern disturbed accordingly to MIPAS pointing performance specifications (dotted line, nearly coinciding with the solid line), and to a scan pattern shifted by 1.5 km with respect to the standard one (dashed line). The differences between the calculated errors are small (very small in the case of the realistic perturbed scan) and considering that the 1.5 km shifted pattern should be an extreme case, we conclude that the dependence of **E** matrix on the measurement grid can be neglected.
The approach of interpolating (linear interpolation in log(p) domain) the **E** matrices computed for the standard MIPAS scan pattern to the actual scan was also tested and it was found to provide unacceptably inaccurate results. This is due to the fact that interpolation necessarily introduces a smoothing in the p,T error propagation matrices which, on the other hand, may have, as in the case of CH_4, very sharp features that are connected to the sequence of the measurements and the corresponding microwindow selection rather than to the atmospheric altitudes.

6. CONCLUSIONS

Propagation of p,T error on to VMR is a significant error component in MIPAS retrievals, therefore it must be carefully evaluated. An algorithm for accurate determination of this error component was proposed. The algorithm uses pre-tabulated matrices that provide the operator of the transformation of the contingent p,T error into a VMR error. In this approach the variability of p,T error propagation as a function of atmospheric conditions is handled by tabulating the p,T error propagation matrix in a 30-degrees latitude grid. It was found that, using standard atmosphere models, this tabulation reproduces quite accurately (within a few percents) the p,T induced error. It is not possible to state whether in practical applications the 30-degrees tabulation step is sufficient, since this depends very much on the relative contribution of p,T induced error to the total VMR error budget, whose estimate depends in turn on some contingent choices that are still pending.
The dependence of the p,T error propagation on season and atmospheric model was also tested. It was found that this dependence can probably be neglected since in a range of cases the estimated p,T induced error varies by less than 20 %. In case this is a too large contribution to the total VMR error budget, a tabulation of the p,T error propagation matrix in the domain of both latitude and season may be considered.

It was also found that for scan patterns deviating from the nominal scan by a realistic amount, the dependence of p,T error propagation on the observation geometry can be neglected still maintaining good accuracy.

REFERENCES

Anderson G.P., S.A.Clough, F.X.Kneizys, J.H. Chetwynd, E.P. Shettle, AFGL Atmospheric Constituent Profiles (0-120 km) – AFGL-TR-86-0110, AD A175173 (1986)

Carlotti M., Applied Optics **27**, 3250-3254 (1988)

Carlotti M., and M. Ridolfi, Applied Optics **38**, 2398-2409 (1999)

Clarmann T.v., A. Linden, G. Echle, A. Wegner, H. Fischer, M. Lopez-Puertas, Proc. IRS '96: 'Current Problems in Atmospheric Radiation', Smith and Stamnes (Eds.), ISBN 0-937194-39-5, Deepak Publishing, 557-560 (1997)

Clarmann T.v., A. Dudhia, G. Echle, J.-M. Flaud, C. Harrold, B. Kerridge, K. Koutoulaki, A. Linden, M. Lopez-Puertas, M. A. Lopez-Valverde, F.J. Martin-Torres, J. Reburn, J. Remedios, C. D. Rodgers, R. Siddans, R. J. Wells and G. Zaragoza, "Study on the Simulation of Atmospheric Infrared Spectra," Final Report of ESA Contract Number 12054/96/NL/CN (1998)

Clarmann T.v., and G. Echle, Applied Optics **37**, 7661-7669 (1998)

Echle G., T. v. Clarmann, A. Dudhia, M. Lopez-Puertas, F. J. Martin-Torres, B. Kerridge, and J.-M. Flaud, Proc. ESAMS '99, ESTEC-ESA, ISSN 1022-6656, WPP-161, **2,** 481-485 (1999)

Endemann M., Proc. ESAMS '99, ESTEC-ESA, ISSN 1022-6656, WPP-161, **1,** 29-43 (1999)

ESA report: "ENVISAT - MIPAS An Instrument for Atmospheric Chemistry and Climate Research" ESA SP-1229, (2000)

Goldman A., R. S. Saunders, J. Quant. Spectrosc. Radiat. Transfer **21**, 155-162 (1979)

Lachance R.L., Proc. ESAMS '99, ESTEC-ESA, ISSN 1022-6656, WPP-161, **1,** 51-63 (1999)

McKee T.B., R. I. Whitman, J. J. Lambiotte jr., "A technique to infer atmospheric water-vapor mixing ratio from measured horizon radiance profiles," *NASA* TN D-5252 (1969)

National Oceanic and Atmospheric Administration, National Aeronautics and Space Administration, United States Air Force, U.S. Standard Atmosphere, (1976)

Ridolfi M., B.Carli, M.Carlotti, A.Dudhia, J.-M.Flaud, M.Hoepfner, P.E.Morris, P.Raspollini, G.Stiller, R.J.Wells, 'An optimized retrieval model for MIPAS near real-time data processing', Proceedings of Spie, **3501**, 170-185 (1998)

Ridolfi M., B.Carli, M.Carlotti, T.v.Clarmann, B.M.Dinelli, A.Dudhia, J.-M.Flaud, M.Hoepfner, P.E.Morris, P.Raspollini, G.Stiller, R.J.Wells, 'An optimized forward model and retrieval scheme for MIPAS near real time data processing' Will be published in Applied Optics, **39**, No. 8, (2000)

Rodgers C.D., Reviews of Geophysics and Space Physics, **14**, 609 (1976)

Rummukainen, M., I.S.A. Isaksen, B. Rognerud, and F. Stordal, Aglobal model tool for 3-D multi-year stratospheric simulations: Model description and first results, J. Geophys. Res., 1999 (in press)

UARS Validation Special Issue, J. Geophys. Res., volume 101, April 30, 1996

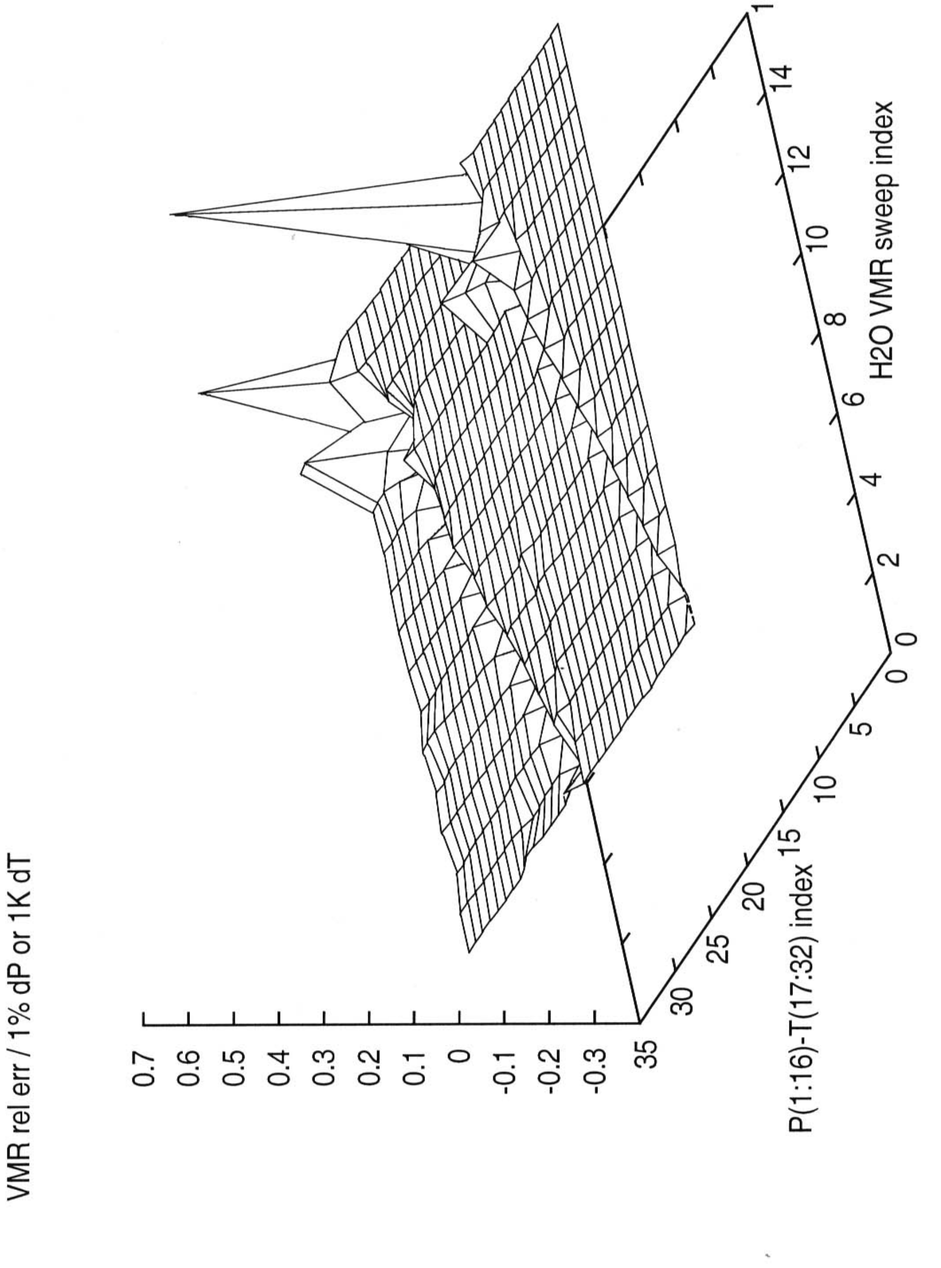

Fig. 1: p,T error propagation matrix for H_2O retrieval. In the horizontal axes: p (1 – 16) and T (17 - 32) retrieved parameters index (left side) and the VMR parameter index (right side). Each index value refers to an altitude in the range 53, …, 8 km in 3 km steps (standard MIPAS scan) with the convention that small index value corresponds to high altitude. Vertical axis: relative VMR error due to 1K temperature error or 1% tangent pressure error.

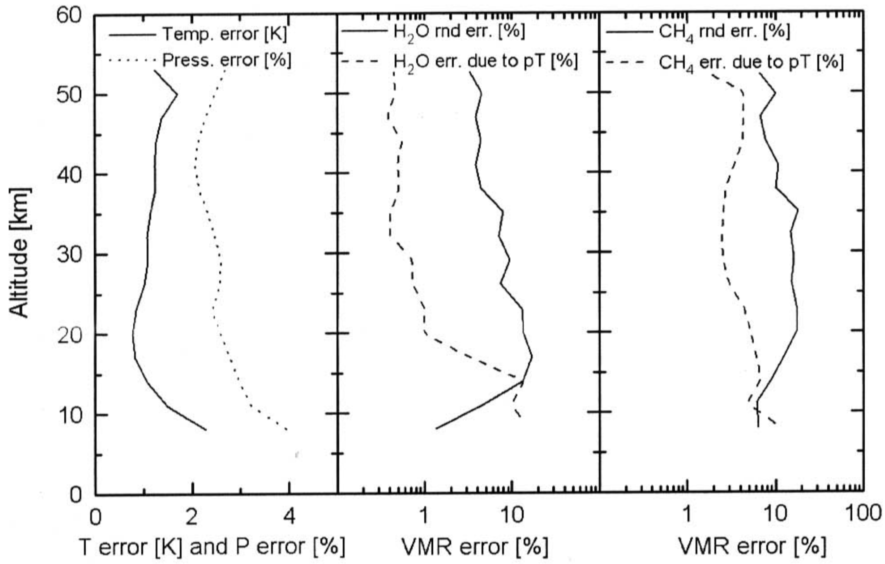

Fig. 2: Right panel: comparison between noise (solid line) and p,T induced (dashed line) errors on the retrieved CH_4 VMR. Center panel: comparison between noise (solid line) and p,T induced (dashed line) errors on the retrieved H_2O VMR. Left panel: p (dashed line) and T (solid line) errors originating the VMR errors reported in the center and right panels.

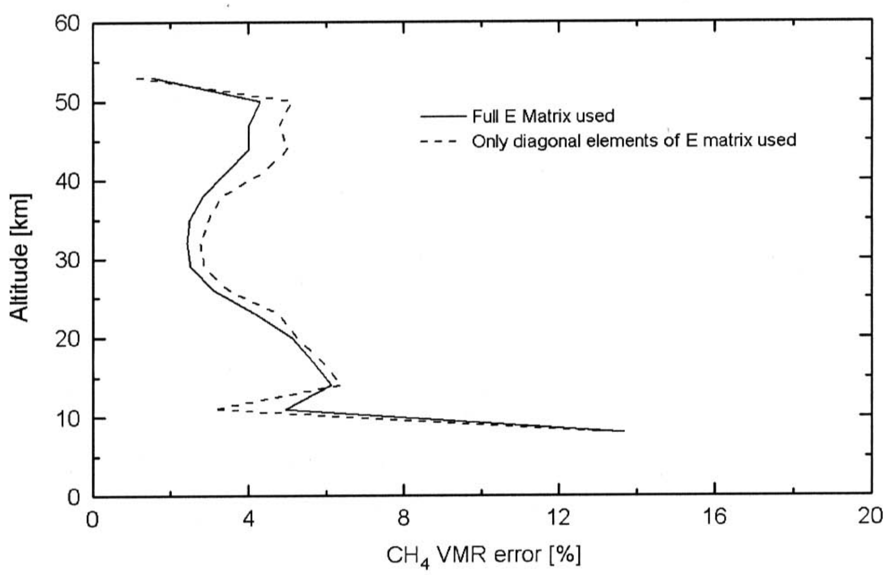

Fig. 3: p,T induced error on the retrieved CH_4 VMR calculated using the full propagation matrix **E** (solid line) and only the elements on the main diagonals of **E** (dashed line).

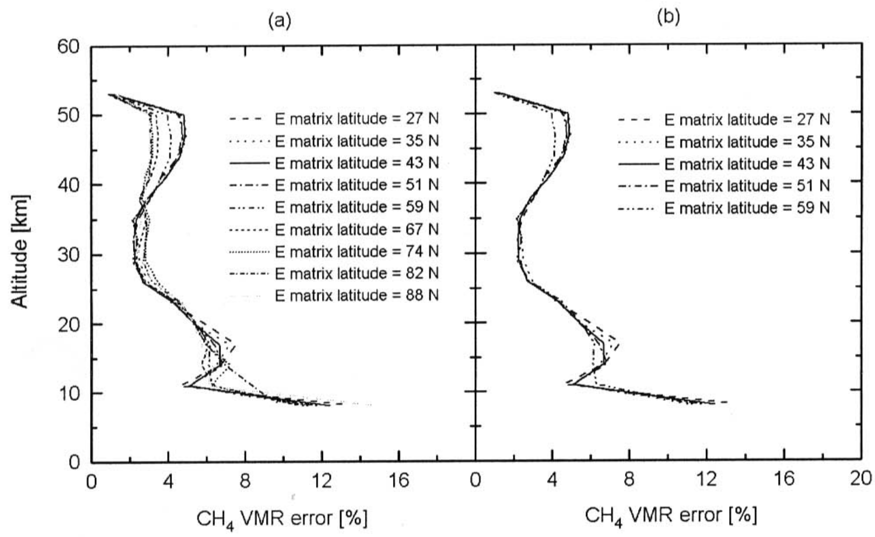

Fig. 4. a): The correct p,T induced error on the retrieved CH_4 VMR (solid line) is compared with the same error obtained using p,T error propagation matrices related to a latitude different from the actual latitude (43° N) of the measurement (dashed lines). The latter errors were calculated using p,T error propagation matrices relating to the latitude range: 27° N - 88° N. b): same as panel a), but p,T error propagation matrices correspond to atmospheres in the latitude range: 27° N - 59° N.

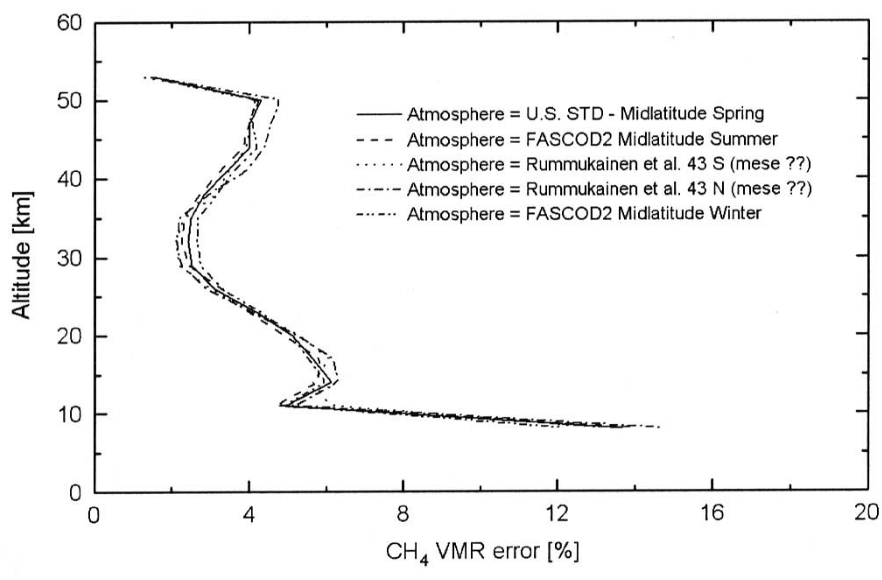

Fig. 5: The correct p,T induced error on the retrieved CH_4 VMR (solid line) is compared with the same error obtained using p,T error propagation matrices related to different atmospheric models (dashed lines).

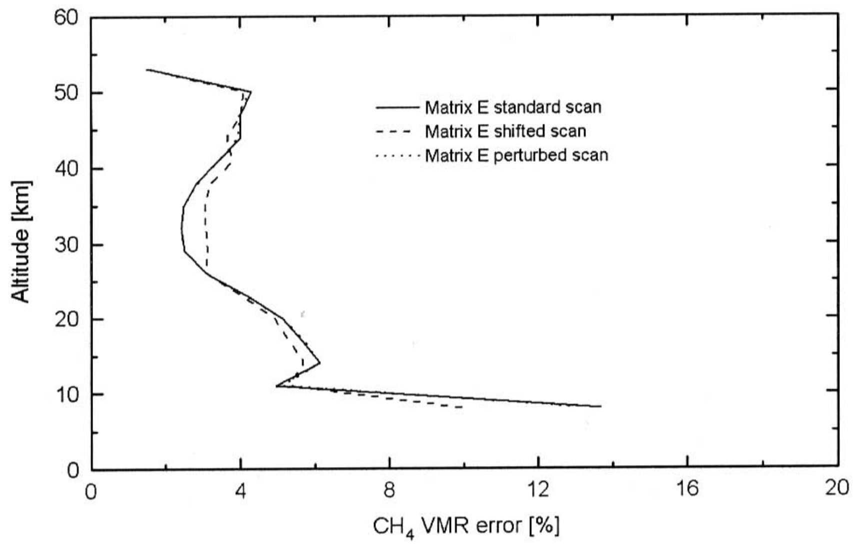

Fig. 6: Comparison of p,T induced error on the retrieved CH_4 VMR calculated using **E** matrices that correspond to different limb-scan patterns. Solid line: standard scan pattern. Dashed line: shifted pattern with an offset of + 1.5 km with respect to the standard. Dotted line: distorted scan pattern with random perturbations consistent with MIPAS pointing system performance.